

# Mineralogical constraints on the paleoenvironments of the Ediacaran Doushantuo Formation

Thomas F. Bristow<sup>a,1</sup>, Martin J. Kennedy<sup>a</sup>, Arkadiusz Derkowski<sup>a</sup>, Mary L. Droser<sup>a</sup>, Ganqing Jiang<sup>b</sup>, and Robert A. Creaser<sup>c</sup>

<sup>a</sup>Department of Earth Sciences, University of California, Riverside, CA 92521; <sup>b</sup>Department of Geoscience, University of Nevada, Las Vegas, NV 89154; and <sup>c</sup>Department of Earth and Atmospheric Sciences, University of Alberta, Edmonton, AB, Canada T6G 2E3

Edited by L. Paul Knauth, Arizona State University, Tempe, AZ, and accepted by the Editorial Board June 22, 2009 (received for review February 4, 2009)

Assemblages of clay minerals are routinely used as proxies for paleoclimatic change and paleoenvironmental conditions in Phanerozoic rocks. However, this tool is rarely applied in older sedimentary units. In this paper, the clay mineralogy of the Doushantuo Formation in South China is documented, providing constraints on depositional conditions of the Ediacaran Yangtze platform that host the earliest animal fossils in the geological record. In multiple sections from the Yangtze Gorges area, trioctahedral smectite (saponite) and its diagenetic products (mixed-layer chlorite/smectite, corrensite, and chlorite) are the dominant clays through the lower 80 m of the formation and constitute up to 30 wt% of the bulk rock. Saponite is interpreted as an *in situ* early diagenetic phase that formed in alkaline conditions ( $\text{pH} \geq 9$ ). The absence of saponite in stratigraphically equivalent basin sections, 200–400 km to the south, indicates that alkaline conditions were localized in a nonmarine basin near the Yangtze Gorges region. This interpretation is consistent with crustal abundances of redox-sensitive trace elements in saponitic mudstones deposited under anoxic conditions, as well as a 10‰ difference in the carbon isotope record between Yangtze Gorges and basin sections. Our findings suggest that nonmarine environments may have been hospitable for the fauna preserved in the Yangtze Gorges, which includes the oldest examples of animal embryo fossils and acanthomorphic acritarchs.

clays | saponite | Neoproterozoic | nonmarine | early animals

Characteristic mudstones, marls, carbonates, and phosphates of the Doushantuo Formation, South China, provide one of the most complete stratigraphic sections through the early Ediacaran Period (635–551 Ma) amenable to geochemical techniques, such as stable isotope studies, used to track paleoenvironmental change (1–3). These sediments encompass rapid climate change at the end of the Cryogenian glacial period (~635 Ma) (4) and an increase in oceanic and atmospheric oxygen levels thought to be a precondition for the development and expansion of animals (5–7). As one of the most famous *Konservat Lagerstätte* of the Ediacaran period, the Doushantuo Formation hosts a fossil record of the diversification of acanthomorphic acritarchs (8), multicellular algae (9), and the appearance of globular microfossils interpreted as embryos of the earliest animals (10, 11).

The Doushantuo Formation is also rich in clay minerals (Fig. 1) and experienced little alteration during burial (4). In post-Mesozoic sedimentary rocks, temporal and spatial trends in assemblages of clay minerals have routinely proved useful indicators of paleoenvironmental conditions, paleoclimatic change, and depositional setting (12, 13). Despite potential transformation during diagenesis and metamorphism, original clay mineral assemblages are also preserved in Precambrian sedimentary rocks (13).

In this paper, we document the clay mineralogy of the Doushantuo Formation with the aim of providing information about the paleoenvironmental conditions in parts of South China during the Ediacaran Period. Interpretations based on mineralogical data are tested with independent geochemical indicators, including the distribution of redox-sensitive elements and C/N ratios of organic

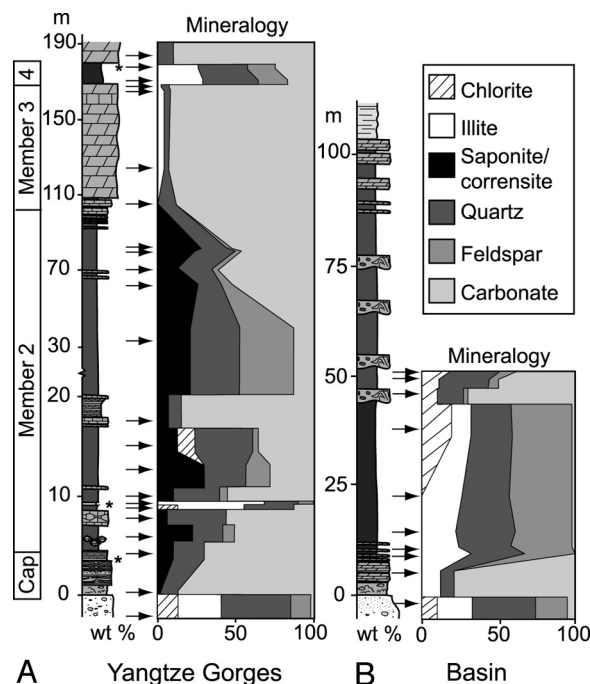


Fig. 1. Mineralogical summary of Doushantuo Formation sections from the Yangtze Gorges area (A) and basin (B), >200 km to the south. Saponite, an indicator of alkaline conditions, is found only in the cap and member 2 mudstones of the Yangtze Gorges sections. Arrows show sampling horizons and asterisks mark the position of ash beds.

matter. Our findings have implications for the depositional setting in which early animals were preserved and interpretations of stable isotope data.

**Geological Background.** Isolated outcrops of the Doushantuo Formation are distributed across a large part of South China, recording sedimentation in the deep basin between the Cathaysian and Yangtze blocks in the southeast, and the broad shelves in the interior of the Yangtze craton in the north and west (Fig. S1). Details of the paleogeography and tectonic setting are still debated and are described in greater detail elsewhere (e.g., refs. 14, 15). Some of the thickest sections of the Doushantuo Formation (up to

Author contributions: T.F.B. and M.J.K. designed research; T.F.B., A.D., G.J., and R.A.C. performed research; M.J.K. and R.A.C. contributed new reagents/analytic tools; T.F.B., M.J.K., A.D., and M.L.D. analyzed data; and T.F.B. wrote the paper.

The authors declare no conflict of interest.

This article is a PNAS Direct Submission. L.P.K. is a guest editor invited by the Editorial Board.

<sup>1</sup>To whom correspondence should be sent at the present address: Division of Geological and Planetary Sciences, California Institute of Technology, 1200 East California Boulevard, Pasadena, CA 91125. E-mail: tbristow@caltech.edu.

This article contains supporting information online at [www.pnas.org/cgi/content/full/0901080106/DCSupplemental](http://www.pnas.org/cgi/content/full/0901080106/DCSupplemental).

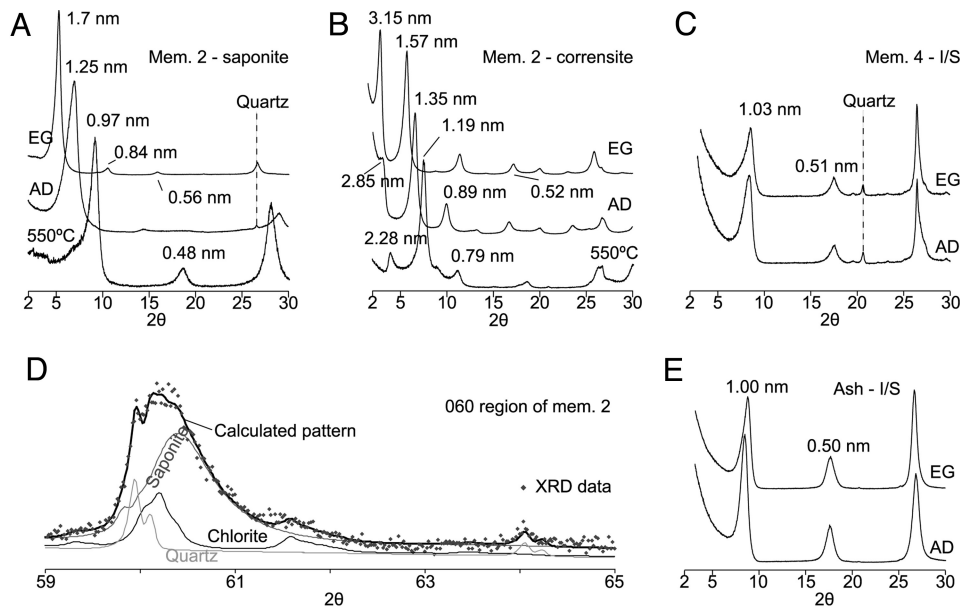


**Fig. 2.** XRD patterns of orientated and random preparations of clay extracted ( $<0.5 \mu\text{m}$ ) from representative Doushantuo Formation samples. (A and B) Glycolated (EG), air-dried (AD), and heated ( $550^\circ\text{C}$ ) patterns of Na-saturated, orientated, preparations of saponite and corrensite-rich samples of member 2. Sample 61104-41 and 61104-7B were collected at 4.5 m and 23 m, respectively. (D) The 060-region of an XRD pattern from a randomly orientated saponite and corrensite bearing clay fraction (sample 61805-20 collected at 80 m) of member 2 with peak position indicative of trioctahedral occupancy. The modeled pattern shown was generated by Rietveld refinement using a mixture of structural models for discrete chlorite and saponite. Note also the presence of trace amounts quartz. (C and E) show glycolated (EG) and air-dried (AD) patterns of orientated preparations of Na-saturated, highly illitic I/S extracted from member 4 mudstone and the ash layer in member 2.

$\sim 200$  m) were deposited in the intra-shelf basins on the Yangtze block, as exemplified by sediments in the Eastern Yangtze Gorges region (1, 8, 14). In this area the formation is typically described in terms of 4 lithologically defined members, shown in Fig. 1 and described in more detail in the *SI Text*. Stratigraphic thickness and lithology show considerable lateral variation and this scheme is not applicable in sections 10s of km away (1, 14). However, it provides a convenient framework to discuss results from the Yangtze Gorges.

In this study, the mineralogy and geochemistry of samples from the Yangtze Gorges area are compared with deeper water basin deposits from Hunan Province. This serves to test the paleogeographic extent of the conditions implied by these proxies. Basin section samples come from Siduping and a section near Huaihua, 200 and 400 km to the south of the Yangtze Gorges, respectively (Fig. S1), where the Doushantuo Formation is thinner ( $\sim 100$  m) and more siliciclastic rich in the lower part (Fig. 1). In some paleogeographic reconstructions it is proposed that basin deposits are separated from an intra-shelf basin in the Yangtze Gorges by a barrier complex (14) (Fig. S1).

**Mineralogy in the Yangtze Gorges Region.** The clay mineral assemblage of the cap carbonate (member 1) and member 2 in the Yangtze Gorges sections is distinctive when compared with clays extracted from the underlying Nantuo diamictite, member 4 mudstones in the same region, and stratigraphically equivalent mudstones immediately overlying the cap carbonate in basin sections (Fig. 1 and Fig. S1). Smectite is the dominant clay mineral in the majority of samples from member 2 in the Yangtze Gorges area. XRD patterns of air dried, Na-saturated, orientated aggregates of the  $<0.5\text{-}\mu\text{m}$  size fraction show a broad peak at 1.25 nm that expands on glycolation to 1.7 nm and collapses on heating at  $550^\circ\text{C}$  to 0.97 nm (Fig. 2A). In patterns of randomly orientated clay extracts a major peak at 0.1538 nm in the 060-region indicates that smectite is trioctahedral (Fig. 2D) (16). This is confirmed by elemental analysis of clay-sized fractions

extracted from smectite-rich samples (Table S1). The high magnesium content ( $\sim 27$  to  $29$  wt% MgO) and smaller amounts of aluminum ( $\sim 7$  to  $9$  wt%  $\text{Al}_2\text{O}_3$ ) in the purest smectite fractions are typical of saponite (12).

Randomly interstratified chlorite/saponite and corrensite—a regular interstratification of smectite (in this case saponite) and chlorite, is found in the cap carbonate and mudstones from the lower part of member 2. Corrensite is identified by a distinctive peak at 3.13 nm and rational series of higher order reflections in XRD patterns of ethylene glycol saturated orientated clay aggregates (Fig. 2B). After heating to  $550^\circ\text{C}$  the 001 peak position shifts to 2.27 nm because of collapse of smectitic layers. The series of basal reflections is nonrational in the heated XRD pattern indicating that chlorite/smectite layers are not perfectly ordered (Fig. 2B). Mg-rich chlorite is also found in some clay fractions of the cap carbonate, occurring as the main clay phase or mixed with corrensite (see Table S1 for chemical analysis).

In all sections of the Doushantuo Formation studied in the Yangtze Gorges (Table S2 lists locations), saponite and corrensite are the dominant clay phases in the cap carbonate and member 2. Quantitative mineralogical analyses show that these trioctahedral clays make up to 30 wt% of the whole rock and  $>50$  wt% of silicate material (Fig. 1 and Table S2). Qualitative examination of orientated XRD patterns of clay aggregates show that corrensite and chlorite are most abundant in the cap carbonate and mudstones at the base of member 2, with a proportional increase of saponite up-section.

Using SEM, clays in mudstones from member 2 exhibit random particle orientations preserved in an open (porous) fabric (Fig. S2B) (17). Clays are often concentrated in subparallel layers and form polygonal networks strung around larger grains (Fig. S2A). These are interpreted as sedimentary textures modified by authigenic mineral growth and/or compaction. Rare spherical ‘rosettes’ of trioctahedral clays have platy dolomite overgrowths (Fig. S2C).

### Mineralogy of Basin Sections and Member 4 in the Yangtze Gorges.

Smectite is absent in stratigraphically equivalent basin mudstones interbedded with and overlying the cap carbonate (Fig. 1). An asymmetric, broadened, peak at approximately 1.0 nm in orientated slides of the clay fraction of selected samples show that highly illitic mixed-layer illite/smectite (I/S), or mixtures of I/S and illite are the only clays (18). The same clay mineral assemblage is found in member 4 mudstones and rare argillaceous partings between carbonate beds in member 3 from the Yangtze Gorges sections (Figs. 1 and 2C).

**Diagenetic Pathways.** The degree to which clays in discrete, thin (<5 cm), ash layers in the Yangtze Gorges have been illitized provides a useful control on the thermal history (i.e., the magnitude and duration of heating) of different parts of the formation. The clay fraction of ash layers from the base and the top of the formation both consist of illitic mixed-layer I/S (Fig. 2E), resulting from illitization of early diagenetic dioctahedral smectite during burial (18). This indicates that the whole formation ( $\approx 200$ -m thick) experienced a similar thermal history during burial diagenesis and is consistent with a maximum burial depth of 4 km for Neoproterozoic strata in the Yangtze Gorges area (19). Moreover, this implies that the switch in clay mineralogy from members 2 to 4 resulted from a change in sedimentary source or paleoenvironmental conditions, rather than by thermal alteration that selectively affected a particular stratigraphic horizon. Mixed-layer I/S from member 4 was likely deposited as detrital dioctahedral smectite or I/S and was illitized to a similar degree as the clays in ash layers.

Smectites that persist in the Doushantuo Formation are a result of enhanced thermal stability of trioctahedral versus dioctahedral smectites. Trioctahedral saponite forms corrensite (regularly interstratified chlorite/smectite) and chlorite during diagenesis (18), and these minerals are now found in certain horizons of the lower Doushantuo Formation. In contrast, dioctahedral smectite and smectitic I/S are illitized to more illitic mixed-layer I/S and illite (12, 18). Experimental synthesis and stability studies indicate that compositional and crystallographic characteristics of trioctahedral smectites make them more thermally stable than the dioctahedral types (18, 20). The local chemical environment is also probably an important control on the degree of diagenesis of saponite (e.g., ref. 21). The variation in the amounts of saponite, corrensite and chlorite observed at different stratigraphic horizons in the lower part of the Doushantuo Formation may be governed by the lithology of the host rock influencing fluid composition.

**Trace-Element Abundances.** The enrichment of redox-sensitive elements, such as Mo, Re, U, and V, in sediments typically occurs under low oxygen and high sulfide levels in the sediment and water column, but is ultimately limited by the supply of these elements (22). Therefore the concentration of these elements may serve as an independent indicator of a particular depositional environment. For example, oxygen depleted conditions in upwelling zones impinging on continental margins act as a trap for redox-sensitive elements, concentrating them through resupply by marine waters (23). However, restricted anoxic basins such as the Black Sea, and anoxic continental lacustrine deposits exhibit significantly lower enrichments of these elements because of a limited supply by the local catchment (Table S3). Despite degree of pyritization (DOP) measurements indicating comparable dysoxic to anoxic conditions during deposition of members 2 and 4 of the Doushantuo Formation in the Yangtze Gorges, the concentration of redox-sensitive elements in these members is strikingly different (Fig. 3 and Fig. S3). Member 2 mudstones contain crustal abundances of Mo, Re, U, and V, whereas member 4 is enriched by 1 to 2 orders of magnitude with respect to member 2 (Fig. 3 and Fig. S3). Plots of TOC vs. trace element

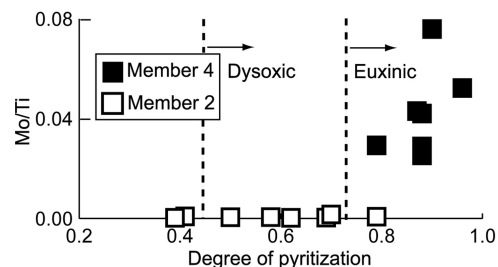


**Fig. 3.** Plot showing depletion of redox-sensitive Mo (normalized to titanium) in member 2 mudstones, despite DOP measurements indicative of oxygen-depleted conditions that typically result in enrichment in a marine setting (23). DOP values >0.45 indicate dysoxic conditions and >0.75 indicate euxinia (47).

concentrations, normalized to Ti, show that changes in TOC content and siliciclastic sedimentation rate between members 2 and 4 were a secondary control on elemental concentrations (Fig. S3). This suggests that an external change in sources or sinks is responsible for these trends. Mo and V enrichment in mudstones above the cap in basin sections support this hypothesis because they contain concentrations more typical of open marine settings (Table S3). Organic-rich samples from member 2 also have distinctive high C/N ratios compared with samples from member 4 (Fig. S4).

**Origin of Saponite.** In the Phanerozoic, saponite formation is limited to specific depositional environments including: weathering profiles developed on Mg-rich rocks, such as basic or ultrabasic igneous rocks and chloritochists, hydrothermal settings where fluids interact with Mg-rich igneous material, as well as alkaline lakes and evaporative basins (12, 13, 18). Several of these possibilities can be ruled out based on the sedimentology, mineralogy, and the depositional history of the Doushantuo Formation.

Saponite and its diagenetic products, make up to 30 wt% of the total sediment and are the dominant (>90 wt%) clay minerals through 80 m of the lower 2 members of the Doushantuo Formation. Therefore invoking a detrital origin for saponite requires an almost exclusive source of clay from a saponite generating weathering profile, or from an older saponite/chlorite deposit, that must be sustained for millions of years. There are basic and ultrabasic rocks found in South China that may have provided a potential source. However, they were intruded and extruded during the Neoproterozoic rift phase, 10s of millions of years before the deposition of the Doushantuo Formation, and are concentrated along margins of the Yangtze block 100s of km away from the Yangtze Gorges region (24). Furthermore, there are no mineralogical indicators of inputs from weathering of mafic or ultramafic rocks. Fe-rich 2:1 clays, like nontronite and Fe-rich beidellite that commonly form with saponite in these types of weathering profiles (18) are not detected in saponitic Doushantuo Formation rocks. Additionally, no mafic minerals are detected with XRD (Table S2) or with SEM. The underlying glacial Nantuo Formation, that blanketed most of South China before deposition of the Doushantuo Formation, is the most likely source of reworked sediments and does not contain saponite. The dominant clay mineral in the Nantuo Formation is dioctahedral illite. In summary, the monomineralic nature of the clay assemblage and lack of an external saponite source makes a purely detrital origin unlikely.

A hydrothermal origin for saponite is inconsistent with the passive tectonic setting proposed for the Doushantuo Formation (15). Furthermore, there is no textural or mineralogical evidence of hydrothermal activity. Hydrothermal saponite forms coatings on other mineral grains, inside veins and replaces mafic minerals (18, 25). It may be accompanied of other secondary Fe and

Mg-rich minerals including celadonite, talc, nontronite and metal oxide/sulfides (12). These textures and minerals are not found in saponitic rocks from the Yangtze Gorges.

**Implications for Paleoenvironmental Conditions.** Exclusion of a hydrothermal and a detrital source, combined with textural evidence, indicates that the Doushantuo Formation saponite formed in situ during early diagenesis. Saponite is part of a group of Mg-rich clay minerals that also includes palygorskite, sepiolite and stevensite, commonly formed in alkaline or evaporative sedimentary basins (*SI Text* and *Table S4*). These clays form either by direct precipitation (neof ormation) or transformation of precursor clays through addition of Mg and Si (*SI Text*). Saponite is typically interpreted to form by transformation because it contains significant amounts of Al (18). This reaction only occurs under specific chemical conditions and can therefore be used as an indicator of pore water chemistry and conditions in the overlying water column during the deposition of members 1 and 2 of the Doushantuo Formation in the Yangtze Gorges (*Table S4*, *Table S5*, and *SI Text*).

Thermodynamic stability diagrams provide a possible guide to the conditions in which saponite formation is favorable. However, discrepancies between conditions in natural systems where saponite occurs and thermodynamic predictions indicate that factors controlling reaction kinetics are a critical concern. For instance, saponite is thermodynamically stable in modern seawater and can be synthesized under equivalent conditions in the lab (26). Despite this, detrital 2:1 dioctahedral clays in modern ocean basins are not transformed into saponite or other Mg-rich clays and are not in thermodynamic equilibrium with seawater (27). The factors influencing the kinetics of formation of trioctahedral Mg-rich clays are poorly understood in natural systems (28). Therefore, we surveyed the chemical conditions in modern environments in which trioctahedral smectites form as a guide to the paleoenvironmental conditions of saponite-bearing sections of the Doushantuo Formation (summarized in *Tables S4* and *S5*).

The vast majority of concentrated, laminated, trioctahedral smectite deposits form in alkaline lacustrine settings (*Tables S4* and *S5*). Modern closed lakes in which trioctahedral smectite form, are characterized by pH values  $>9$ , low Mg concentrations (of a few ppm), and variable Si concentrations ranging from 10s to 100s ppm (*Table S5*). High pH ( $\sim 9$  or higher) appears to be crucial for the production of trioctahedral smectites at appreciable rates (20, 28).

Saponite is also observed forming at moderate pH (of  $\approx 8$ ) in organic lean sediments of evaporitic mudflats, recharged by seawater in the Salina Ometepe, Baja California. In this setting saponite production is induced by Mg concentrations an order of magnitude greater than in seawater (29). However, sedimentary and lithological features of saponite-bearing, organic-rich mudstones and marls of the Doushantuo Formation are not consistent with a transient evaporitic setting capable of concentrating Mg. The prevalence of mm-scale parallel laminations, limited evidence of current reworking, and the absence of subaerial exposure features indicate deposition below wave base (1, 8). Furthermore, the absence of evaporites argues against elevated Mg concentrations inducing saponite formation.

The Ediacaran Period is widely regarded as a transitional time in terms of ocean chemistry. Therefore the possibility that Ediacaran seawater favored the formation of saponite should be considered. Strongly alkaline conditions, posited as characterizing the period after the Marinoan glaciation, could potentially explain short-term precipitation of early diagenetic clays for tens to hundreds of thousands of years (ref. 30 and references therein). However, the predominance of saponite through 80 m of sedimentary section above the cap carbonate in the Doushantuo Formation indicate the persistence of alkaline conditions that cannot be attributed to geochemical perturbations related to deglaciation.

The spatial and temporal restriction of saponite to the Yangtze Gorges area is inconsistent with the idea of widespread conditions promoting saponite formation. Coeval mudstones from basin sections do not contain saponite (Fig. 1). The clay fraction is mainly made up of dioctahedral illitic I/S, a common detrital mineral in marine sediments. Furthermore, saponite and other early diagenetic Mg-rich clay minerals have not been reported from Ediacaran aged marine sedimentary rocks in other parts of the world. These observations suggest the development of an isolated alkaline basin in the Yangtze Gorges area.

Independent constraints on ocean chemistry also indicate that the high pH and Mg concentrations required for saponite to form are unlikely to characterize Ediacaran seawater. A global ocean at pH  $>9$ , the threshold for trioctahedral smectite formation in modern lacustrine systems (*Table S5*), would be in equilibrium with atmospheric  $p\text{CO}_2$  levels well below the 90-ppm threshold thought to induce the runaway ice-albedo of snowball earth events and is unfeasible in the postglacial world (30, 31). Ediacaran seawater with Mg concentrations an order of magnitude greater than modern seawater is inconsistent with the marine evaporite record (32).

Finally, it should be noted that, if the formation of early diagenetic Mg-rich clays were found to be widespread in the Ediacaran oceans, it would have profound implications for the budgets of several geochemical cycles including Mg, Si, and C, and as a result the  $p\text{CO}_2$  levels in the atmosphere and feedbacks regulating climate (33). In this way, our favored interpretation, that the Doushantuo Formation saponite represents localized alkaline conditions, is parsimonious.

Isolation of the Yangtze Gorges area from the open ocean during deposition of members 1 and 2 of the Doushantuo Formation may also help explain trace element and carbon isotope trends. Typical Proterozoic Mo concentrations in marine organic-rich shales of 24 ppm (34) are comparable with concentrations in organic-rich mudstones above the cap in basin sections (avg. 30 ppm,  $n = 10$ ; *Table S3*). However, these concentrations are an order of magnitude greater than crustal abundances found in anoxic mudstones of member 2 in the Yangtze Gorges (avg. 2.5 ppm,  $n = 8$ ). Other redox-sensitive elements (Re, U, and V) are also anomalously low in saponite-bearing parts of the Yangtze Gorges sections. This depletion may be indicative of limited supply from the local catchment and the absence of links to the large reservoir of the global ocean.

Carbon isotope profiles from the lower Doushantuo Formation also show regional differences of up to 10‰. Isotopic values of  $\sim +5‰$  characterize much of member 2 in the Yangtze Gorges compared with values of between  $-4$  and  $-6‰$  in strata overlying the cap in basin sections (3). Assuming isotope values are a primary signal, this difference is interpreted as representing an isotopic gradient of 10‰ between surface and deep ocean waters (3). In this model, the negative carbon isotope values, characteristic of deep anoxic waters, are a result of enhanced remineralization of organic matter (3). Our data does not bear on a stratified ocean model, however, it suggests an alternative explanation in which the distinct isotopic signal observed in member 2 in the Yangtze Gorges is simply the result of a lack of connectivity with the basin and the different isotopic controls characteristic of a nonmarine system.

**Distribution of Fossils.** Member 2 in the Yangtze Gorges hosts multiple acanthomorphic and leiospherid acritarch fossils (1, 8). Acanthomorphic acritarchs are only found in Ediacaran age sedimentary rocks and identifiable by their large size and complex morphology. The widespread distribution of the group as a whole is used to support a marine interpretation and  $\approx 40\%$  of acanthomorphic species from the Doushantuo Formation have been identified in Ediacaran sections on other paleocontinents (35). However, by definition acritarchs are a group of

organisms whose taxonomic affinity and ecological niche is uncertain. Leiosphaerid acritarchs, abundant in member 2 of the Doushantuo Formation, are proposed to be among the earliest organisms adapted to freshwater/brackish conditions during the Precambrian (36). Furthermore, comparisons of the well documented acanthomorph records from Australia and China show disparities in the timing of appearance and the fauna that make up these fossil assemblages. Only 5 of 60 taxa are shared between these areas and acanthomorphs preserved in the Doushantuo Formation appear as much as 50 million years earlier than in Australia (37). It is posited that these differences stem from the specialized environments of the Doushantuo Formation (37). Certain acanthomorphic acritarchs, more recently termed large ornamented Ediacaran microfossils (LOEMs), are interpreted as resting stages of Metazoa offspring (38). They are proposed as an evolutionary adaptation to anoxic conditions thought to prevail for prolonged periods on shallow marine shelves in the Ediacaran (38). Such an adaptation would also be advantageous to animals living in nonmarine settings, which are characterized by fluctuating environmental conditions.

It is possible that these fossils indicate periodic marine incursions into the Yangtze Gorges area during the deposition of member 2, but geochemical, mineralogical, and sedimentological evidence do not support this interpretation. In fact the reestablishment of an oceanic link during member 3 is implied by enrichment of member 4 shales in Mo, Re, U, and V by 1 to 2 orders of magnitude with respect to member 2 and a complete change in the clay mineral assemblage. The contrasting C/N ratios of organic bearing mudstones from member 2 to 4 are also consistent with nonmarine vs. marine values from Phanerozoic sediments (39). This may indicate a switch in the source of organic material, although the composition of terrigenous organics in the Ediacaran is poorly constrained.

## Conclusions

Several genera of fossils, interpreted as animal embryos, are hosted in sedimentary sections of the Doushantuo Formation in the Yangtze Gorges area (1, 8, 11). Clay mineral data show that these fossil-bearing rocks were deposited under alkaline conditions. A marine interpretation for these sections is unfeasible if the chemical conditions in modern sedimentary environments where Mg-rich trioctahedral smectites form are taken as constraints. Moreover, several lines of evidence are consistent with the interpretation that parts of the Doushantuo Formation represent an isolated nonmarine basin, including: the spatial and temporal restriction of saponite, lack of redox-sensitive trace element enrichment in demonstrably anoxic sediments, and distinctive C/N ratios of organic matter in saponitic mudstones.

This interpretation has two major implications. The first is that cap carbonates may have a broader range of depositional environments than currently assumed, including nonmarine settings for some examples. This is suggested by presence of trioctahedral clay minerals within cap carbonates and the absence of evidence of depositional hiatus between the cap carbonate and member 2 mudstones in the Yangtze Gorges (19). Cap carbonate formation within an evaporative glacial lake has previously been proposed for the Marinoan examples in central Australia based on similarities of their distinctive features with Holocene Antarctic dry lakes (40). Broadly synchronous carbon isotopic trends in cap carbonates deposited in marine and nonmarine settings could be explained by a common atmospheric source of  $^{13}\text{C}$ -depleted carbon such as methane (4, 41).

Our data also implies that nonmarine environments may have been hospitable for early animals. The isolation of this basin and its unusual chemistry may help explain the endemism of

elements of the Doushantuo fauna and their preservation by silica permineralization. Early silicification and development of fossiliferous cherts should be promoted by increased silica concentration under elevated pHs indicated by saponite. A probable nonmarine origin for early animals is also consistent with the hypothesis that the Precambrian ocean was a challenging place for early metazoans to develop because it was more saline than in the Phanerozoic and as a result contained less dissolved oxygen (42). Our study demonstrates that clay minerals provide an overlooked Ediacaran paleoenvironmental proxy that may be useful in identifying other nonmarine deposits to help test this hypothesis.

Finally, it is worth considering that our data represents a single shelf-to-basin transect of the Doushantuo Formation; further work is required to characterize the extent of alkaline conditions in South China. The depositional setting of the famous phosphatic fossil localities in Weng'an county, approximately 700 km to the southwest, that host similar animal, acritarch and algal assemblages as sections in the Yangtze Gorges, is of particular interest (10, 35).

## Materials and Methods

The Doushantuo Formation was logged and sampled at Jiulongwan, Huajipo, Sixi, Jiuqunao, Siduping, and a section near Huaihua. The location of these sections and stratigraphic position of sampling are listed in Table S2.

**Mineral Quantification and Clay Mineral Analysis.** A Kratos XRD-6000 with Cu-tube was used for XRD analyses. Mineral quantification was carried out on powdered samples spiked with 10% ZnO. This mixture was homogenized in McCrone mill with methanol, dried and side loaded into a holder for random orientation (43). XRD patterns were measured between  $2-65^\circ 2\text{-theta}$ . BGMN, a Rietveld refinement program (44), and Quanta (Chevron) a modified RIR/MIF full-pattern fitting program, were used for mineral quantification. Errors are estimated at  $\pm 10\text{ wt}\%$  for clays and  $\pm 5\text{ wt}\%$  for major mineral constituents from tests on artificial mixtures.

The discussion of clay mineralogy presented in this paper is based on XRD and compositional analysis of 30 clay-size fractions extracted from representative samples. Extraction involved carbonate removal, organic matter decomposition and Fe and Mn (oxy)hydroxide removal from sample powders (45). The  $<0.5\ \mu\text{m}$  size fraction was separated by centrifuge, washed, and dried on glass slides from suspensions, before measuring the  $1.5$  and  $30^\circ 2\text{-theta}$  range after air drying and saturation with ethylene glycol. Some fractions were side-loaded to observe the *hkl* series of peaks and determine octahedral occupancy. Polished and broken sample chips were examined using the SEM to study paragenesis and mineral textures. Bulk elemental analysis of clay extracts mounted on conductive tape was carried out using energy dispersive system (EDS) analysis.

**Trace Element Determination.** Trace element determinations were made using a Perkin-Elmer 6100 ICP MS instrument at the University of Alberta after digestion of shale samples using  $\text{Na}_2\text{O}_2$  sintering (46). Repeated measurements of 100 ppb solutions for Mo, Ti, V, and U show  $<2\%$  deviation in accuracy from true values for all elements except U (with 5% deviation). For Re, repeated measurements of a 100 ppt solution show  $<8\%$  deviation in accuracy from true values. Precision expressed as Relative Standard Deviation (RSD%) based on 5 replicate measurements of 100 ppb or 100 ppt (Re) solutions is  $<1\%$  for all elements except U and Re (1.2% and 1.5%, respectively).

**Total Organic Carbon (TOC) Content and Carbon/Nitrogen Ratio.** Total carbon and nitrogen contents of powdered samples, dried for 12 h at  $80^\circ\text{C}$ , were measured on Thermo-Finnegan Flash EA1112 nitrogen/carbon analyzer. Repeated measurements of an aspartic acid standard indicate reproducibility of  $<5\%$  for carbon and  $<3\%$  for nitrogen. Total carbonate carbon was determined by measuring pressure change after acidification of samples with 20% HCl inside sealed glass tubes. Carbonate content is calculated from calibration curves prepared using known quantities of standard dolomite and limestone. TOC is calculated by subtracting total inorganic carbon from total carbon.

**Degree of Pyritization.** Degree of pyritization is defined as the ratio  $\text{Fe}_p/(\text{Fe}_p + \text{Fe}_H)$ , where  $\text{Fe}_p$  is pyrite Fe and  $\text{Fe}_H$  is HCl-extractable Fe (47).  $\text{Fe}_p$  was determined using chromium reduction (48). Samples were boiled for 2 h in

a solution of HCl and reduced chromium and continuously flushed with nitrogen gas. Sulfur was collected as zinc sulfide by bubbling gas through zinc acetate trap solution and quantified by titrating acidified trap solution with KI, using starch indicator to show the end point. Extractions of fresh ground pyrite standard show  $98 \pm 1\%$  sulfur recovery. To determine Fe<sub>H</sub>, samples were warmed (60 sec), then boiled (60 sec) in concentrated HCl, before quenching the reaction and diluting the solution with deionised water. Settled sample solutions and standards were mixed with ferrozine reagent and hydroxylamine HCl, and total Fe concentration was measured using a spectrophotometer.

**ACKNOWLEDGMENTS.** We thank T. Lyons for discussions and use of laboratory facilities; S. H. Zhang and H. C. Wu for field assistance and logistical support; D. Mrofka and K. Morrison for laboratory assistance; K. Gray, N. J. Butterfield, S. Xiao, R. Kleeberg, R. Raiswell, S. Severmann, C. Scott, B. Jones, and D. Pevear for advice and comments; and R. Ferrell and numerous anonymous reviewers for constructive reviews of this manuscript. This work was supported by Geological Society of America student research grant (to T.F.B.), National Aeronautics and Space Administration Exobiology Grant NNG04GJ42G, and National Science Foundation Division of Earth Sciences Grants 0345207 and 0345642 (to M.J.K.).

- McFadden KA, et al. (2008) Pulsed oxidation and biological evolution in the Ediacaran Doushantuo Formation. *Proc Natl Acad Sci USA* 105:3197–3202.
- Condon D, et al. (2005) U-Pb ages from the Neoproterozoic Doushantuo Formation, China. *Science* 308:95–98.
- Jiang G, Kaufman AJ, Christie-Blick N, Zhang S, Wu H (2007) Carbon isotope variability across the Ediacaran Yangtze platform in South China: Implications for a large surface-to-deep ocean  $\delta^{13}C$  gradient. *Earth Planet Sci Lett* 261:303–320.
- Jiang G, Kennedy MJ, Christie-Blick N (2003) Stable isotopic evidence for methane seeps in Neoproterozoic postglacial cap carbonates. *Nature* 426:822–826.
- Canfield DE, Poulton SW, Narbonne GM (2007) Late Neoproterozoic deep-ocean oxygenation and the rise of animal life. *Science* 315:92–95.
- Knoll AH (2003) *Life on a Young Planet: The First Three Billion Years of Evolution on Earth* (Princeton Univ Press, Princeton, NJ).
- Kennedy MJ, Droser ML, Mayer LM, Pevear D, Mrofka D (2006) Late Precambrian oxygenation: Inception of the clay mineral factory. *Science* 311:1446–1449.
- Zhou C, Xie G, McFadden K, Xiao S, Yuan X (2007) The diversification and extinction of Doushantuo-Pertataka acritarchs in South China: Causes and biostratigraphic significance. *Geol J* 42:229–262.
- Xiao S, Yuan X, Steiner M, Knoll AH (2002) Macroscopic carbonaceous compressions in a terminal Proterozoic shale: A systematic reassessment of the Miaohu biota, South China. *J Paleontol* 76:347–376.
- Xiao S, Zhang Y, Knoll AH (1998) Three-dimensional preservation of algae and animal embryos in a Neoproterozoic phosphorite. *Nature* 391:553–558.
- Yin L, et al. (2007) Doushantuo embryos preserved within diapause egg cysts. *Nature* 446:661–663.
- Weaver CE (1989) *Clays, Muds, and Shales* (Elsevier, Amsterdam).
- Chamley H (1989) *Clay Sedimentology* (Springer, Berlin).
- Vernhet E (2007) Paleobathymetric influence on the development of the late Ediacaran Yangtze platform (Hubei, Hunan, and Guizhou provinces, China) *Sediment Geol* 197:29–46.
- Jiang GQ, Sohl LE, Christie-Blick N (2003) Neoproterozoic stratigraphic comparison of the Lesser Himalaya (India) and Yangtze block (south China): Paleogeographic implications. *Geology* 31:917–920.
- Moore DM, Reynolds RC (1997) *X-ray Diffraction and the Identification and Analysis of Clay Minerals* (Oxford Univ Press, New York).
- O'Brien NR, Slatt RM (1990) *Argillaceous Rock Atlas* (Springer, New York).
- Meunier A (2005) *Clays* (Springer, Berlin).
- Jiang GQ, Kennedy MJ, Christie-Blick N, Wu HC, Zhang SH (2006) Stratigraphy, sedimentary structures, and textures of the late Neoproterozoic Doushantuo cap carbonate in south China. *J Sediment Res* 76:978–995.
- Velde B (1985) *Clay Minerals: A Physico-chemical Explanation of Their Occurrence* (Elsevier, Amsterdam).
- Sandler A, Nathan Y, Eshet Y, Raab M (2001) Diagenesis of trioctahedral clays Miocene to Pleistocene in a sedimentary-magmatic sequence in the Dead Sea Rift, Israel. *Clay Miner* 36:29–47.
- Algeo TJ (2004) Can marine anoxic events draw down the trace element inventory of seawater? *Geology* 32:1057–1060.
- Brumsack HJ (2006) The trace metal content of recent organic carbon-rich sediments; implications for Cretaceous black shale formation. *Palaeogeogr Palaeoclimatol Palaeoecol* 232:344–361.
- Li ZX, et al. (2003) Geochronology of Neoproterozoic syn-rift magmatism in the Yangtze Craton, South China and correlations with other continents: Evidence for a mantle superplume that broke up Rodinia. *Precambrian Res* 122:85–109.
- Setti M, Marinoni L, Lopez-Galindo A (2004) Mineralogical and geochemical characteristics (major, minor, trace elements and REE) of detrital and authigenic clay minerals in a Cenozoic sequence from Ross Sea, Antarctica. *Clay Miner* 39:405–421.
- Decarreau A (1980) Experimental crystallogeneses of Mg-smectite: Hectorite, stevensite. *Bull Miner* 103:579–590.
- Eberl DD (1984) Clay mineral formation and transformation in rocks and soils. *Philos Trans R Soc* 311:241–257.
- Deocampo DM (2005) Evaporative evolution of surface waters and the role of aqueous CO<sub>2</sub> in magnesium silicate precipitation: Lake Eyasi and Ngorongoro Crater, northern Tanzania. *S Afr J Geol* 108:493–504.
- Hover VC, Walter LM, Peacor DR, Martini AM (1999) Mg-smectite authigenesis in a marine evaporative environment, Salina Ometepe, Baja California. *Clays Clay Miner* 47:252–268.
- Fairchild IJ, Kennedy MJ (2007) Neoproterozoic glaciation in the earth system. *J Geol Soc* 164:895–921.
- Bristow TF, Kennedy MJ (2008) Carbon isotope excursions and the oxidant budget of the Ediacaran atmosphere and ocean. *Geology* 36:863–866.
- Holland HD (1978) *The Chemistry of the Atmosphere and Oceans* (New York, Wiley).
- Mackenzie FT, Garrels RM (1966) Chemical mass balance between rivers and oceans. *Amer J Sci* 264:507–525.
- Scott C, et al. (2008) Tracing stepwise oxygenation of the Proterozoic ocean. *Nature* 452:456–459.
- Zhang Y, Yin L, Xiao SH, Knoll AH (1998) Permineralized fossils from the Terminal Proterozoic Doushantuo Formation, South China. *Paleontological Society Memoir* 50:1–52.
- Martin-Closas C (2003) The fossil record and evolution of freshwater plants: A review. *Geol Acta* 1:315–338.
- Grey K (2005) Ediacaran palynology of Australia. *Memoirs Assoc Australasian Palaeontol* 31:1–439.
- Cohen PA, Knoll AH, Kodner R (2009) Large spinose microfossils in Ediacaran rocks as resting stages of early. *Proc Natl Acad Sci USA* 106:6519–6524.
- Tyson RV (1995) *Sedimentary Organic Matter: Organic Facies and Palynofacies* (Chapman & Hall, London).
- Walter MR, Bauld J (1983) The association of sulphate evaporites, stromatolitic carbonates and glacial sediments: Examples from the Proterozoic of Australia and the Cainozoic of Antarctica. *Precambrian Res* 21:129–148.
- Kennedy MJ, Mrofka D, von der Borch C (2008) Equatorial permafrost methane clathrate destabilization as the trigger of snowball Earth deglaciation. *Nature* 453:642–645.
- Knauth LP (2005) Temperature and salinity history of the Precambrian ocean: Implications for the course of microbial evolution. *Palaeogeogr Palaeoclimatol Palaeoecol* 219:53–69.
- Šrodon J, Drits VA, McCarty DK, Hsieh JCC, Eberl DD (2001) Quantitative X-ray diffraction analysis of clay-bearing rocks from random preparations. *Clays Clay Miner* 49:514–528.
- Bergmann J, Friedel P, Kleeberg R (1998) BGMN—a new fundamental parameters based Rietveld program for laboratory X-ray sources, its use in quantitative analysis and structure investigations. *CPD Newsletter* 20:5–8.
- Jackson ML (1969) *Soil Chemical Analysis* (Published by author).
- Longerich HP, Jenner GA, Fryer BJ, Jackson SE (1990) Inductively coupled plasma-mass spectrometric analysis of geological samples: A critical evaluation based on case studies. *Chem Geol* 83:105–118.
- Raiswell R, Buckley F, Berner RA, Anderson TF (1988) Degree of pyritization of iron as a paleoenvironmental indicator of bottom-water oxygenation. *J Sediment Petrol* 58:812–819.
- Canfield DE, Raiswell R, Westrich JT, Reaves CM, Berner RA (1986) The use of chromium reduction in the analysis of reduced inorganic sulfur in sediments and shales. *Chem Geol* 54:149–155.